Int. J. Electrochem. Sci., 5 **(2010)** 478 - 488

International Journal of ELECTROCHEMICAL SCIENCE
www.electrochemsci.org

Kinetic Investigation of $LiCoO_2$ by Electrochemical Impedance Spectroscopy (EIS)

Jishi Zhao, Li Wang, Xiangming He, Chunrong Wan, Changyin Jiang*

Institute of Nuclear & New Energy Technology, Tsinghua University, Beijing 100084, PR China
*E-mail: hexm@tsinghua.edu.cn

Received: 24 January 2010 / *Accepted:* 15 April 2010 / *Published:* 30 April 2010

Electrochemical impedance spectroscopy (EIS) is employed to investigate the electrochemical properties of $LiCoO_2$ cathode. At initial state, the Nyquist plots consist of one compressed semicircle in high and intermediate frequency ranges that reflect charge transfer resistance and a straight line inclined at a constant angle to the real axis in lower frequency range that reflects the diffusion properties of lithium ion in solid materials. When the cell was charged for several hours, the Nyquist plots consist of two compressed semicircles alike in appearance of a half ellipse at high and intermediate frequency ranges and an anomalous line at lower frequency range, and the shape of the second semicircle is a half ellipse in appearance almost. The information of electrolyte resistance, surface film resistance and charge transfer resistance have been obtained by modeling with two different equivalent circuits according with the Nyquist plots with different shape. It can be speculated that both the passivating film on the surface of $LiCoO_2$ cathode and the channels for lithium ion transfer in $LiCoO_2$ cathode are mostly formed during the first charge/discharge process. Both diffusion coefficient of lithium ion in $LiCoO_2$ cathode and exchange current density are in accord with the analysis of the Nyquist plots of electrochemical impedance spectra, indicating the rationality of the speculation.

Keywords: EIS; kinetic properties; $LiCoO_2$; Lithium-ion batteries

1. INTRODUCTION

Although widely used in various portable electric devices as a power supply, lithium ion batteries have still attracted much attention in attempts to ameliorate the performance. In recent years, many research groups have applied electrochemical impedance spectroscopy (EIS) to study the kinetics of promising electrode materials for rechargeable lithium batteries [1-2]. Among these materials such as $LiFePO_4$ [3-4], $LiCoO_2$ [4-5] and $LiMn_2O_4$ [6-7] have been characterized extensively because of their high reversibility in Li-ion intercalation/de-intercalation processes.

So far, most of studies were carried out on composite electrodes [8-10] and thin-film electrodes [11-12], a single particle of micrometer size electrodes were also investigated with the aim of clarifying its electronic and ionic transport properties [13]. Results deduced with composite electrodes are influenced by not only the electrochemical properties of the active materials but also the fabrication (*i.e.* organic binder, conductive additives, and porosity.) It is important to know the kinetic properties of lithium transport in the oxide host to determine the cycling performance, so, the stability of oxide during the charge/discharge process is desirable to be studied to enhance the performance of lithium ion batteries.

Electrochemical impedance spectroscopy (EIS) technique has been used to studied the electrode materials because it can reveal the relationship between the crystal lattice with the electrochemical properties [14-15]. In this work, we report the electrochemical investigations on $LiCoO_2$ cathode by EIS technique. Particularly, we demonstrate here that impedance of $LiCoO_2$ cathode changed with cycles increasing, which help us to know the influence of the impedance of electrode on its cycling performance. Both the apparent chemical diffusion coefficient of lithium ion (D_{Li^+}) in $LiCoO_2$ cathode and the exchange current density (j_0) were obtained from the analysis of impedance spectra.

2. EXPERIMENTAL PART

In present work, the $LiCoO_2$ particles are prepared based on controlled crystallization and solid state reaction. And the particles are spherical; the results of X-ray Diffraction show that there is no impurity in the particles accord with the JCDS standard. Moreover, the size distribution of particles is between 7um and 12um. It should be mentioned that the sample has been used widely in commercial lithium ion batteries. This is different from the previous work. For electrochemical performance evaluation, half-cell studies were performed. The $LiCoO_2$ powder was mixed with acetylene black and PTFE dissolved in ethanol in the weight ratio of 8:1:1 to form slurry. After solvent evaporation, the electrode was pressed and dried at 120^{o}C under vacuum over 24 h. CR2025-type coin cells were assembled in a glove box (M. Braun GmbH, Germany) with H_2O and O_2 content below 1 ppm. Metallic lithium foil was used as counter electrode. The electrolyte was 1.0 M $LiPF_6$ dissolved in a mixture of ethylene carbonate (EC), ethyl methyl carbonate (EMC) and dimethyl carbonate (DMC) (1:1:1, v/v) and Celgard 2400 polyethylene was used as the separator.

EIS was done using the ZAHNER-IM6eX electrochemical workstation (Germany) at room temperature. The EIS measurements were performed with 10 mV perturbation amplitude in the range from 100 kHz to 5 mHz in automatic sweep mode from high to low frequencies. The impedance spectra were recorded at each state allowing at least 5 additional hours for equilibration after each charging/discharging step. The counter electrode was lithium foil about 1.0 cm^2 and the electrochemical measurements were performed with a two-electrode system. The counter electrode is large enough, so it almost does not affect the EIS behavior. Data acquisition and analysis were done, respectively, using the electrochemical impedance software.

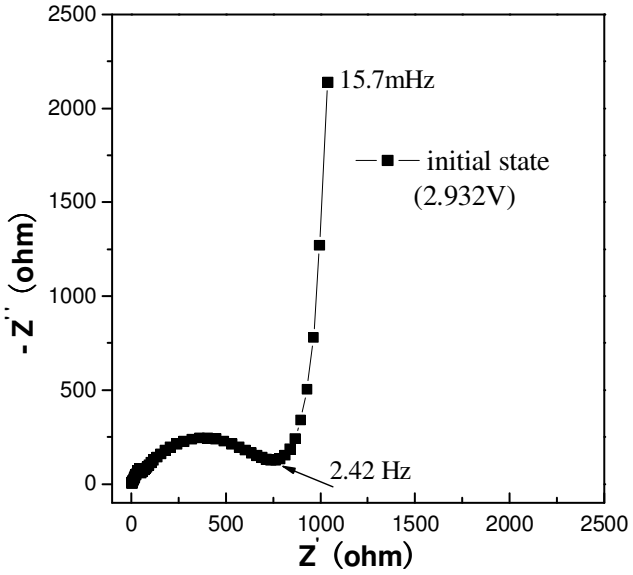

Figure 1. -Nyquist plots of $LiCoO_2$ cathode at the initial state (0% SOC) of the first charge/discharge cycle

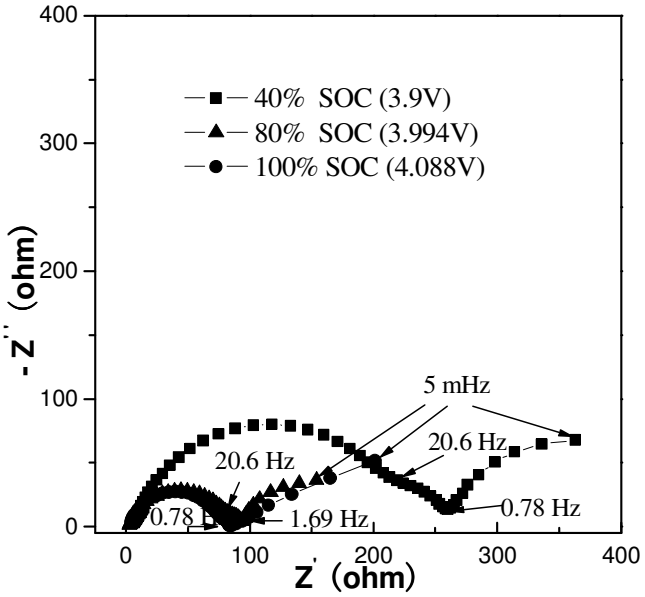

Figure 2. -Nyquist plots of $LiCoO_2$ cathode electrode at different SOC in the first charge/discharge cycle

3. RESULTS AND DISCUSSION

3.1. Analysis of the electrochemical impedance spectra

Fig. 1 and Fig. 2 display the -Nyquist plots of the EIS obtained from the $LiCoO_2$ cathode at the initial state and at different state of charge (SOC) in the first charge/discharge process, respectively. As

shown in Fig. 1, the -Nyquist plots consist of an out-of-shaped semicircle alike in appearance of a half ellipse in high and intermediate frequency ranges and a straight line inclined at a constant angle to the real axis in the lower frequency range at the initial state with open circuit voltage of 2.932V. However, the Nyquist plots at different SOC are different from that at the initial state. There are two anomalous semicircles with compressed shape in high and intermediate frequency ranges and an anomalous line in the lower frequency range, and the shape of the second semicircle is a half of an ellipse almost.

Moreover, another effect to be noticed is the large difference in impedance response between Fig.1 and Fig.2. This difference is basically in the lowest frequency semicircle of the dispersion, which shows an increasing tendency to close to the real axis (Z') as the voltage increases. Since the interface between the current collector and the $Li_{1-x}CoO_2$ cathode is blocking for lithium ions, the imaginary part of Z (Z'') would tend to be infinity as the frequency tends to zero. The fact that the semicircle however tends to close to the real axis (Z') can reasonably be explained by the change of the electronic conductivity of $Li_{1-x}CoO_2$ with x. Indeed, this assumption is supported by some literatures, which demonstrates that the material passes from an insulator when x is close to unity, to a conductor when x assumes lower value [16-19]. By the way, the analysis for the impedance spectra will be done to explain this phenomenon in the latter section.

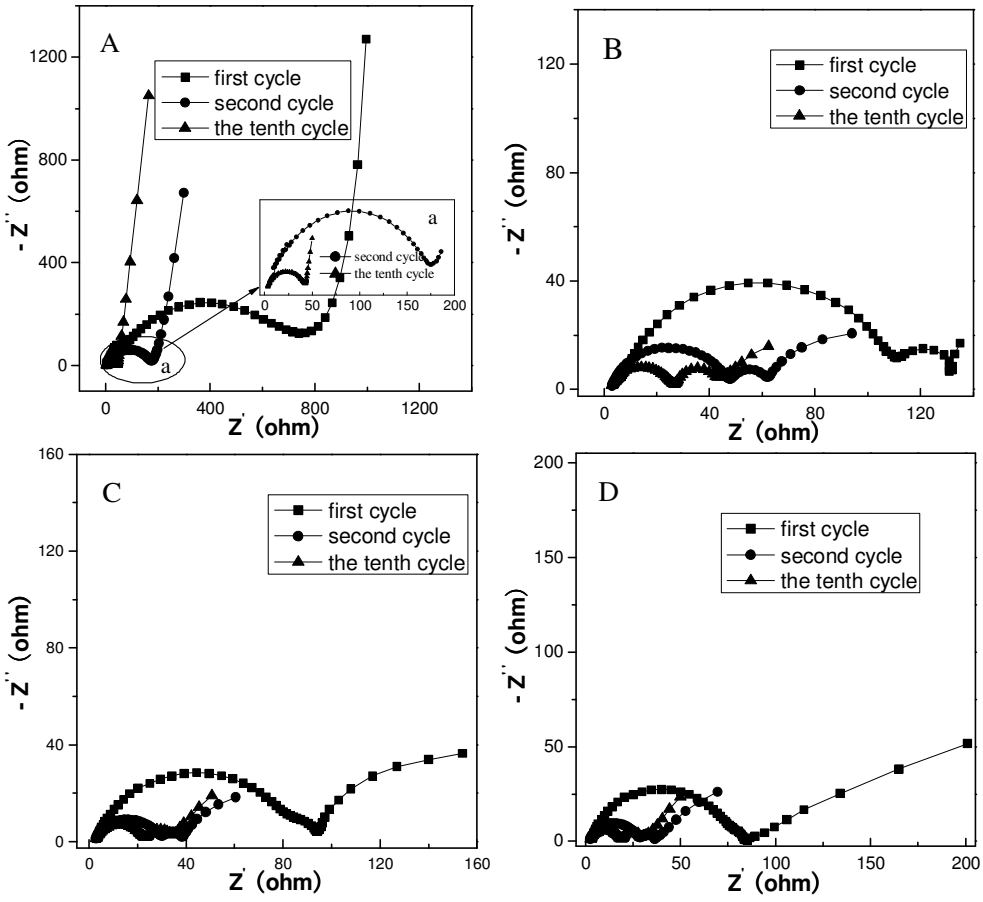

Figure 3. -Nyquist plots of $LiCoO_2$ cathode at different cycle (A: initial state; B: 40% SOC; C: 80% SOC; D: 100% SOC)

Also, it can be found that the semicircles appeared in the high frequency range show no obvious changes with the SOC increasing from 80% to 100%, which reveals that the passivating film is stable. The radius of the semicircle appeared in moderate frequency range decrease with the voltage increasing, revealing that the decreasing of the charge-transfer resistance. One reason applied to explain the phenomena is that the ionic conductivity of the cathode materials increases with the SOC increasing.

Fig.3 displays the electrochemical impedance spectra of the $LiCoO_2$ cathode in different cycles at initial state, 40% SOC, 80% SOC and full charged state, respectively. From Fig. 3A to Fig. 3D, we found that the shape of the -Nyquist plots are alike for different cycles. That is, the -Nyquist plots for the initial state at different cycle consist of one semicircle at high frequency range and a line at lower frequency range; and the -Nyquist plots at 40% SOC, 80% SOC and full charged consist of two anomalous semicircles with compressed shape in high and moderate frequency range and a anomalous line at lower frequency range. Also, the radius of the semicircle decrease with the cycle increasing. Moreover, the difference in radius between the first cycle and the second circle is larger than that between the second cycle and the tenth cycle, revealing that the passivating film forms mostly during the first charge/discharge process and is stable during the latter charge/discharge cycles. Obviously, comparing with the increasing cycle, the state of charge (SOC) has much more influence on the impedance after the first charge/discharge cycle.

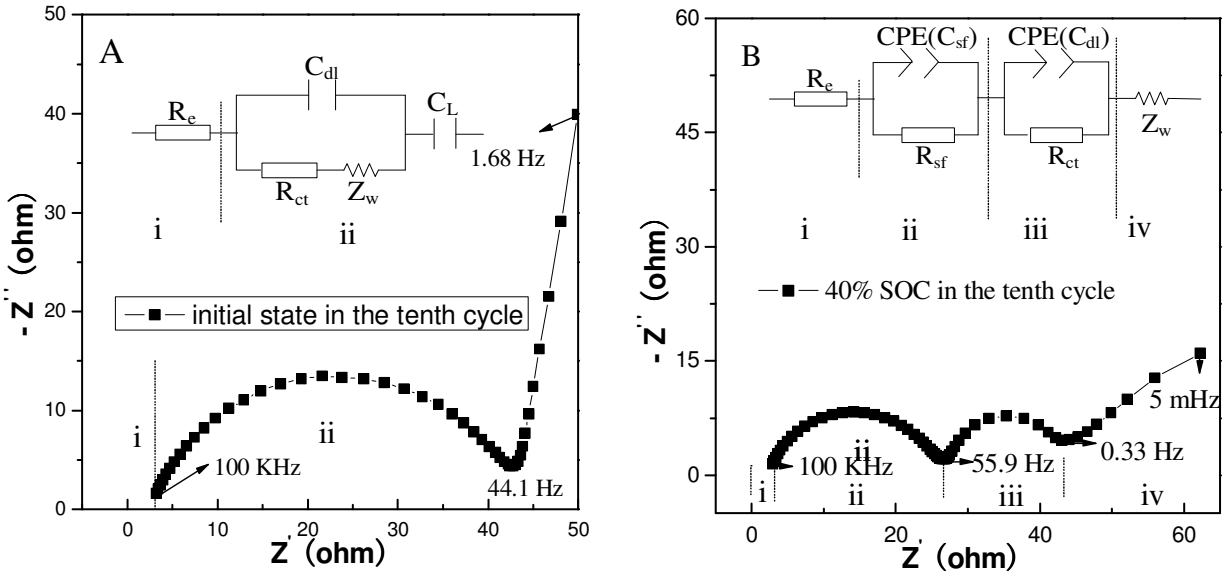

Figure 4. EIS plots of $LiCoO_2$ cathode at different state of charge (SOC) in the 10^{th} cycle and their equivalent circuits (A: initial state; B: 40% SOC)

In order to investigate the changes in the EIS spectra of $LiCoO_2$ electrode during the charging process in detail, we employed equivalent circuits displayed in Fig. 4 to analyze the impedance spectra data shown in Fig. 3. For the $LiCoO_2$ cathode at the initial state in the 10^{th} cycle (with 0% SOC),

typically one dispersed semicircle within the frequency range (100K Hz-44.1 Hz) was observed (see Fig. 4A). The equivalent circuit is given in Fig. 4A as an insert. The total impedance could be regarded as the electrolyte resistance R_e and the charge transfer resistance R_{ct}, and C_{dl} is the double-layer capacitance. Z_w is the Warburg impedance that reflects the diffusion of lithium-ion in the solid. C_L means simply the intercalation capacitance. As shown in Fig. 4B, when $LiCoO_2$ electrode was charged at 0.1C rate to 40% SOC, the shape of the impedance spectra changed totally, and two semicircles were observed. In other words, the semicircle at high-frequency range (100K Hz-55.9 Hz) and the semicircle at lower frequency range (55.9 Hz-0.33 Hz) are separated. The semicircle at high frequency can be ascribed to the electrolyte resistance and the surface film impedance (represented by $R_e(R_{sf} \| CPE(C_{sf}))$), and the semicircle at lower frequency can be ascribed to the lithium-intercalation process (represented by $R_{ct} \| CPE(C_{dl})$), the approximate beeline closed to the second semicircle (in the frequency range of 0.33 Hz-0.005 Hz) reveals the diffusion of lithium-ion in the $LiCoO_2$ cathode, which can be represented by Z_w series to the others parts in the equivalent circuit given in the insert of Fig. 4B. It should be mentioned that the constant phase element (CPE) has been introduced in equivalent circuit B instead of pure capacitive element C_{sf} and C_{dl}. Though the equivalent circuit simulated by the electrochemical impedance software is different from the previous research [14-15], it can match the measurement results totally. In others cycles, the shape of the impedance spectra and their equivalent circuit are the same as that shown in Fig. 4. The fitting results, including R_e, R_{sf} and R_{ct}, are summarized in Fig. 5.

Fig. 5a, Fig. 5b and Fig. 5c display the variation of R_e, R_{sf} and R_{ct} with potential, respectively. From Fig. 5a, it can be found that R_e at initial state (with 0% SOC) decreases with cycle increasing, revealing that the charge/discharge process enhance the transference performance of lithium-ion in the electrolyte. R_e decreases with SOC increasing in every cycle, and there is no obvious differences at the same SOC in every cycle after the cell charged to 40% SOC. Obviously, comparing with the increasing cycles, the state of charge (SOC) has more impact on R_e. Fig. 5b displays the relationship between R_{sf} and the SOC in different charge/discharge cycles, which reveals that R_{sf} at the first charge/discharge process with 40% SOC is much larger than that of others. In the first charge/discharge process, R_{sf} decreases sharply from 54 Ω cm^{-2} to 4.15 Ω cm^{-2} with the SOC increases from 40% to 80%. The SOC has no evident influence on R_{sf} in the second and tenth charge/discharge process. It is speculated that the passivating surface film of the cathode is mainly formed during the forepart in the first charge/discharge process, and then keeps stable in the subsequent cycles. Moreover, the contact performance between electrolyte and cathode electrode at the beginning of the charging process should be also considered, which has been proposed by Holzapfel et al. [20] during the research on the first lithiation and charge/discharge cycles of graphite materials. Fortunately, the analysis results of R_{sf} is in accord with the inferences for Fig. 1 and Fig. 2 in above sections. As shown in Fig. 5c, the trend of charge transfer resistance R_{ct} *vs* SOC is the same with that of R_{sf} *vs* SOC, indicating that the channels for lithium-ion transfer in $LiCoO_2$ cathode is mainly formed during the first charge/discharge process, and then change little in the following charge/discharge processes, making R_{ct} has no evident changes in the tenth cycle.

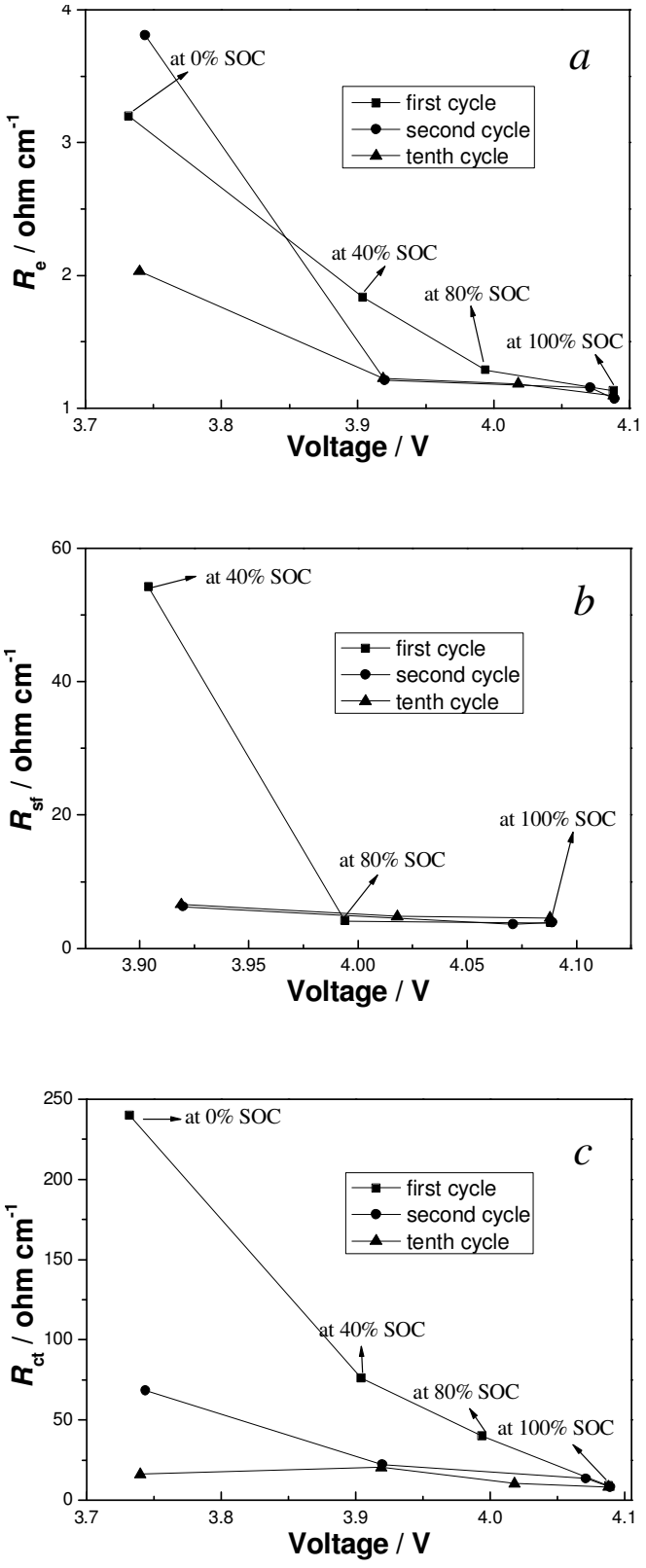

Figure 5. Variation of R_e, R_{sf} and R_{ct} vs. potential

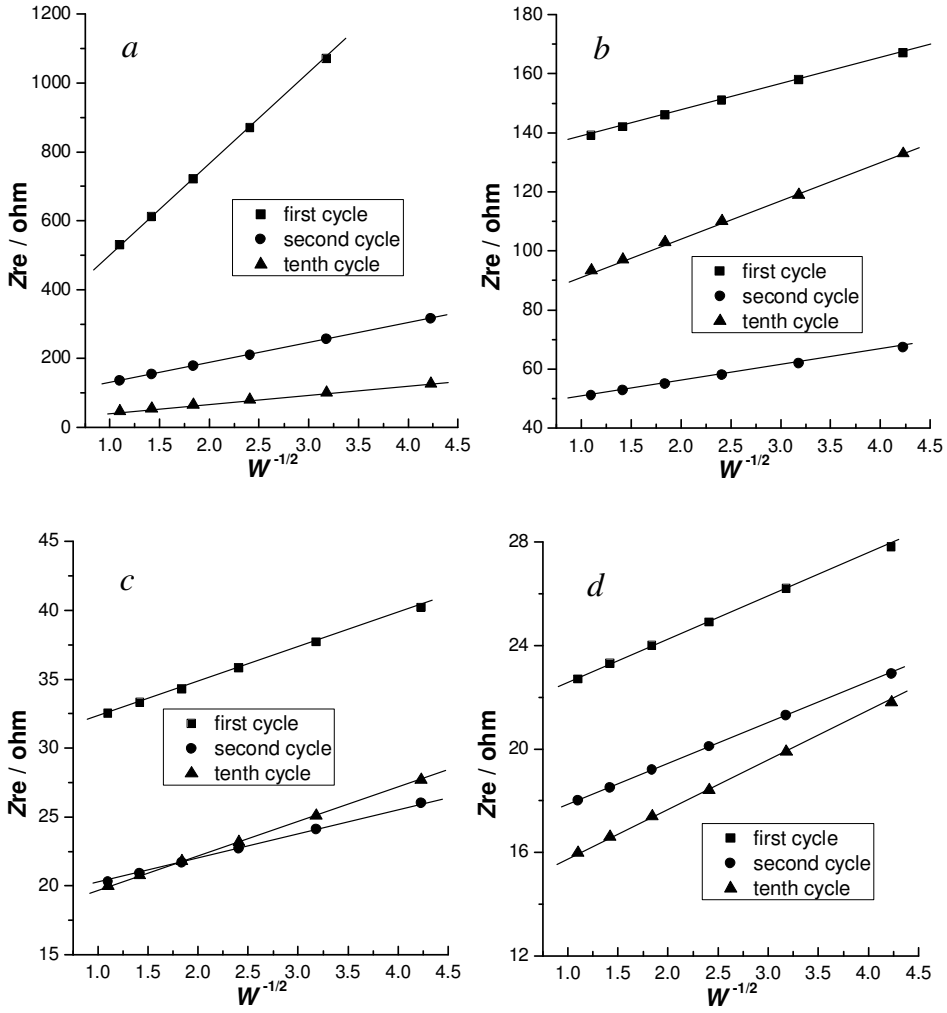

Figure 6. the relationship between $-Z_{re}$ and $\omega^{-1/2}$ at low frequency region (*a*: the initial state at different cycles;

3.2. Diffusion coefficient and exchange current density

The exchange current density and the lithium ion diffusion coefficient can be calculated according to the following equation, respectively:

$$j_0 = \frac{i_0}{A} = \frac{RT}{nFR_{ct}A} \quad (1)$$

$$D_{Li^+} = R^2T^2 / 2A^2n^4F^4C^2\sigma^2 \quad (2)$$

where j_0 and D_{Li^+} are the exchange current density and the diffusion coefficient of lithium ion, respectively. R means the gas constant, T is the absolute temperature (the number is 298.15 in present work), and n is the number of electrons per molecule during oxidization (n=1 according to the

reaction of lithium ion intercalation/de-intercalation), F is the Faraday's constant, A is the area of the cathode/electrolyte interface, it is 0.5 cm^{-2} in this work. The value of R_{ct} is deduced from the modeling of EIS data discussed above. C *is* the concentration of lithium ion, and σ is the Warburg factor which has relationship with Z_{re} ($\omega = 2\pi f$):

$$Z_{\mathrm{re}} = R_{\mathrm{D}} + R_{\mathrm{L}} + \sigma\omega^{1/2} \qquad (3)$$

The relationship between $-Z_{re}$ and square root of frequency ($\omega^{-1/2}$) in low frequency region are shown in Fig. 6 as follows:

The diffusion coefficient of lithium ion (D_{Li^+}) calculated based on equations (2) and (3) [21] was displayed in Table 1. D_{Li^+} increases with the SOC increasing from 0% to 80% in every charge/discharge process, and also increases with the increasing cycles at a given SOC. It also can be found that the difference between the first cycle and the second cycle is more evident than that between the second cycle and the tenth cycle. Croce et al. [22] has proved that the de-intercalation of lithium-ion from the oxide cathode materials reduces the de-intercalation of lithium-ion from oxede cathode material de-shields the electrostatic repulsion between the oxygen of two adjacent layers and expands the crystal lattice, resulting in improving the diffusion properties of lithium-ion in oxide cathode materials. Combination with the results shown in Table 1, it can be speculated that such processes is mostly occurred during the first cycle. The exchange current density (j_0) calculated by equation (1) [13] was also shown in Table 1. Absolutely, comparing with D_{Li^+} , j_0 was influenced by SOC and cycles in the same way. The calculated results indicate that the rationality of the supposition that both the passivating film of $LiCoO_2$ cathode and the channels for lithium-ion transference in $LiCoO_2$ cathode are mainly formed during the first charge/discharge process.

Table 1. The diffusion coefficient of lithium-ion (D_{Li^+}) in cathode and exchange current density (j_0) at different state

Parameters / State	D_{Li^+} / cm^2 S^{-1}			j_0 /A cm^2		
	First cycle	Second cycle	Tenth cycle	First cycle	Second cycle	Tenth cycle
0% SOC	2.11E-18	4.31E-17	2.11E-16	2.14E-04	7.50E-04	0.00315
40% SOC	4.79E-15	6.44E-14	1.42E-13	6.76E-04	0.0023	0.00251
80% SOC	1.32E-13	1.06E-12	1.42E-12	0.00128	0.0038	0.00497
100% SOC	**	**	**	0.0058	0.00613	0.00619

** The value of concentration of lithium ion in oxide cathode is zero at the full-charged state

4. CONCLUSIONS

In attempts to investigate the kinetics properties of $LiCoO_2$ cathode, EIS technique has been employed. The Nyquist plots of electrochemical impedance spectra at initial state in each cycle consists of one semicircle alike in appearance of a half ellipse in high and intermediate frequency ranges and a straight line inclined at a constant angle to the real axis in the lower frequency range. One

more compressed semicircle alike in appearance of a half ellipse appears in high and intermediate frequency ranges after the cell was charged. Corresponding to the different Nyquist plots obtained in EIS measurements, two different equivalent circuits were applied to model the experimental data. The results showed that the electrolyte resistance (R_e) had no obvious change with increasing cycle; both the surface film resistance (R_{sf}) and charge transfer resistance (R_{ct}) decreased with the increasing cycle at the same SOC. In the first charge/discharge process, R_{sf} decreases sharply from 54 ohm cm^{-2} to 4.15 ohm cm^{-2} with the SOC increases from 40% to 80%. Comparing with SOC, cycles had more influence on R_{sf} and R_{ct}, it can be speculated consequently that both the passivating film on the surface of $LiCoO_2$ cathode and the channels for lithium ion transfer in $LiCoO_2$ cathode are mostly formed during the first charge/discharge process. D_{Li^+} and j_0 have been calculated based on the equivalent circuits of electrochemical impedance spectra, both of them increase with the SOC increasing in every cycle, and great changes occurred in the first charge/discharge cycle.

ACKNOWLEDGEMENT
The authors would like to thank the anonymous reviewers for their useful suggestion about the further research on the composite anode. This work was supported by the National Basic Research Program of China (973 Program, project No.:2007CB209705).

References

1. K. M. Shaju, G. V. S. Rao, B. V. R. Chowdari. *Electrochim. Acta*. 48 (2003) 2671.
2. S. Q. Liu, S. C. Li, K. L. Huang, B. L. Gong, G. Zhang. *J. Alloys Compd*. 450 (2008) 499.
3. F. Gao, Z. Y. Tang. *Electrochim. Acta*. 53 (2008) 5071.
4. J. X. Ma, C. S. Wang, S. Wroblewski. *J. Power Sources* 164 (2007) 849.
5. H. W. Yan, X. J. Huang, H. Li, L. Q. Chen. *Solid State Ionics* 113-115 (1998):11.
6. R. Yazami, Y. Ozawa. *J. Power Sources* 153 (2006) 251.
7. A. K. Hjelm, G. Lindbergh. *Electrochim. Acta*. 47 (2002) 1747.
8. G. M. S. R. Thomas, P. G. Bruce, J. B. Goodenough. *J. Electrochem. Soc*. 132 (1985) 1521.
9. G. M. S. R. Thomas, P. G. Bruce, J. B. Goodenough. *Solid State Ionics* 18-19 (1986) 794.
10. M. D. Levi, G. Salitra, B. Markovsky, H. Teller, D. Aurbach, U. Heider, L. Heider. *J. Electrochem. Soc*. 146 (1999) 1279.
11. J. M. McGraw, C. S. Bahn, P. A. Parilla, J. D. Perkins, D. W. Readey, D. S. Ginley. *Electrochim. Acta*. 45 (1999)187.
12. H. Sato, D. Takahashi, T. Nishina, I. Uchida. *J. Power Sources* 68 (1997)540.
13. K. Dokko, M. Mohamedi, Y. Fujita. *J. Electrochem. Soc*. 148 (2001) A422.
14. J. P. Meyers, M. Doyle, R. M. Darling, J. Newman. *J. Electrochem. Soc*. 147(2000) 2930.
15. J. Euler, W. Nonnenmacher. *Electrochim. Acta*. 2 (1960) 268.
16. F. Croce, A. Deptula, W. Lada, R. Marassi, T. Olczak, F. Ronci. *Ionics* 3 (1997) 390.
17. M. D. Levi, G. Salitra, B. Marcowsky, H. Teller, D. Aurbach, U.Heider, L. Heider. 146 (*J. Electrochem. Soc.* 1999) 1279.
18. J. Molenda, A. Stopklosa, T. Bak. *Solid State Ionics* 36 (1989) 53.
19. M. Shibuya, T. Nishina, T. Matsue, I. Uchida. *J. Electrochem. Soc*. 143 (1996) 3157.
20. M. Holzapfel, A. Martinent, F. Alloin, B. LeGorrec, R. Yazami, C. Montella. *J. Electroanal. Chem*. 546 (2003) 41.
21. H. Liu , C. Li , H. P. Zhang, L. J. Fu, Y. P. Wu, H. Q. Wu. *J. Power Sources* 159 (2006) 717.

22. F. Croce, F. Nobili, A. Deptula, W. Lada, R. Tossici, A. D'Epifanio, B. Scrosati, R. Marassi. *Electrochem. Commun*. 1 (1999) 605.